Physics Letters B 741 (2015) 66–70

Contents lists available at ScienceDirect

Physics Letters B

www.elsevier.com/locate/physletb

The role of finite-size effects on the spectrum of equivalent photons in proton–proton collisions at the LHC

Mateusz Dyndal [a,b], Laurent Schoeffel [b,*]

[a] AGH University of Science and Technology, Cracow, Poland
[b] CEA Saclay, Irfu/SPP, Gif-sur-Yvette, France

ARTICLE INFO

Article history:
Received 17 October 2014
Received in revised form 24 November 2014
Accepted 6 December 2014
Available online 11 December 2014
Editor: J.-P. Blaizot

ABSTRACT

Photon–photon interactions represent an important class of physics processes at the LHC, where quasi-real photons are emitted by both colliding protons. These reactions can result in the exclusive production of a final state X, $p+p \to p+p+X$. When computing such cross sections, it has already been shown that finite size effects of colliding protons are important to consider for a realistic estimate of the cross sections. These first results have been essential in understanding the physics case of heavy-ion collisions in the low invariant mass range, where heavy ions collide to form an exclusive final state like a J/Ψ vector meson. In this paper, our purpose is to present some calculations that are valid also for the exclusive production of high masses final states in proton–proton collisions, like the production of a pair of W bosons or the Higgs boson. Therefore, we propose a complete treatment of the finite size effects of incident protons irrespective of the mass range explored in the collision. Our expectations are shown to be in very good agreement with existing experimental data obtained at the LHC.

1. Introduction

A significant fraction of proton–proton collisions at large energies involves quasi-real photon interactions. This fraction is dominated by elastic scattering, with a single Born-level photon exchange. The photons can also be emitted by both protons, where a variety of central final states can be produced. The proton–proton collision is then transformed into a photon–photon interaction and the protons are deflected at small angles. At the LHC, these reactions can be measured at the energies well beyond the electroweak energy scale. This offers an interesting field of research linked to photon–photon interactions, where the available effective luminosity is small, relative to parton–parton interactions, but is compensated by better known initial conditions and usually simpler final states. Indeed, for high energetic proton–proton collisions, at a center of mass energy s, the idea is to search for the exclusive production of a final state X through the reaction $p+p \to p+p+X$. Therefore, the initial state formed by both photons is well-defined, while the final state formed by X with no other hadronic activity is much simpler than in a standard inelastic proton–proton interaction. In the following, we write this reaction as $pp(\gamma\gamma) \to ppX$.

In order to compute the cross section for the process $pp(\gamma\gamma) \to ppX$, we need to consider that each of the two incoming protons emits a quasi-real photon which fuse to give a centrally produced final state X ($\gamma+\gamma \to X$). This calculation relies on the so-called equivalent photon approximation (EPA) [1–5]. The EPA is based on the property that the electromagnetic (EM) field of a charged particle, here a proton, moving at high velocities becomes more and more transverse with respect to the direction of propagation. As a consequence, an observer in the laboratory frame cannot distinguish between the EM field of the relativistic proton and its transverse component, which can be labeled as the transverse EM field of equivalent photons. This implies that the total cross section of the reaction $pp(\gamma\gamma) \to ppX$ can be approximately described as a photon–photon fusion cross section ($\gamma\gamma \to X$) folded with the equivalent photon distributions $f(.)$ for the two protons

$$\sigma(p+p \to p+p+X) = \iint f(\omega_1) f(\omega_2) \sigma_{\gamma\gamma\to X}(\omega_1,\omega_2) \frac{d\omega_1}{\omega_1}\frac{d\omega_2}{\omega_2}, \quad (1)$$

where $\omega_{1,2}$ represent the energies of the photons and are integrated over. For each photon, the maximum energy is obviously the energy of the incident proton $\sqrt{s}/2$. However, there is also the constraint that the highest available energy for one photon is of the order of the inverse Lorentz contracted radius of the proton, γ/r_p, where r_p represents the proton radius. Let us note that

* Corresponding author.
E-mail address: laurent.schoeffel@cea.fr (L. Schoeffel).

http://dx.doi.org/10.1016/j.physletb.2014.12.019

the two photon center-of-mass energy squared is $W^2_{\gamma\gamma} = 4\omega_1\omega_2$, and the rapidity of the two photons system is defined as $y_{\gamma\gamma} = 0.5 \ln[\omega_1/\omega_2]$.

In Eq. (1), the photon distributions $f(.)$ are already integrated over the virtuality ($Q^2_{1,2}$) of the photons. As this dependence is of the order of $1/Q^2_{1,2}$, this justifies the approximation that both photons are quasi-real.

We can remark that for practical issues, the situation may be more complex. Indeed, each proton can either survive and, then, is scattered at a small angle, as considered above. This is the case of elastic emission. Elastic two-photon processes yield very clean event topologies at the LHC: two very forward protons measured away from the interaction point and a few centrally produced particles (forming the final state X). But, it is also possible that one or both protons dissociate into a hadronic state. This is the case of inelastic emission. In this paper, we restrict the discussion to the elastic case.

Let us note also that the calculations presented in this paper are commonly used for heavy-ion collisions, where the EPA approximation can be applied similarly. Only the charges and the radii of the incident particles are modified in this case.

Previous studies have been done using Eq. (1) in order to compute cross sections at LHC energies for various photon–photon processes in proton–proton collisions, $pp(\gamma\gamma) \to ppX$, corresponding to different final states X [6,7]. Some results are displayed in Fig. 1. The exclusive production of pairs of muons and pairs of W bosons have been generated using the Herwig++ generator [8]. The exclusive production of pairs of photons has been generated using the FPMC generator [9] at large $W_{\gamma\gamma}$ where the $\gamma\gamma \to \gamma\gamma$ cross section is dominated by one-loop diagrams involving W bosons [10]. Finally, the exclusive production of the Higgs boson is computed according to higgs effective field theory (HEFT) [11]. Obviously, this last reaction appears as a point in Fig. 1, representing the total cross section, at the Higgs mass.

In this paper, our purpose is to generalize Eq. (1) to the physics case where the impact parameter dependence of the interaction cannot be neglected [12]. In particular, we show that this approach is needed when we take in consideration the finite size of colliding protons (or heavy-ions) in the calculations. This is not new in the sense that these finite size effects have already been encoded in the Starlight Monte Carlo [13] dedicated to heavy-ion collisions. Let us note that Starlight is not restricted to photon–photon interactions but can also be used in photon–Pomeron configurations, as it is done at LHCb [14]. However, Starlight is focused mainly on the low invariant mass domain around the mass of the J/Ψ, which justifies some approximations made for example by neglecting the magnetic form factors.

In the following we develop some calculations that are valid also for the exclusive production of high masses final states in proton–proton collisions, like the production of a pair of W bosons or the Higgs boson. Therefore, our purpose in this paper is to propose a complete treatment of the finite size effects of incident protons irrespective of the mass range explored in the collision. In Section 2, these calculations are presented extensively. Then, results are discussed in Section 3 and compared to existing measurements.

2. Impact parameter dependent equivalent photon method

Deriving the expression of the equivalent photon distribution of the fast moving proton without neglecting the impact parameter dependence means that we determine this distribution as a function of the energy of the photon and the distance $\vec{b}$ to the proton trajectory. This distance is defined in the plane transverse to the proton trajectory. Therefore we speak of transverse distance.

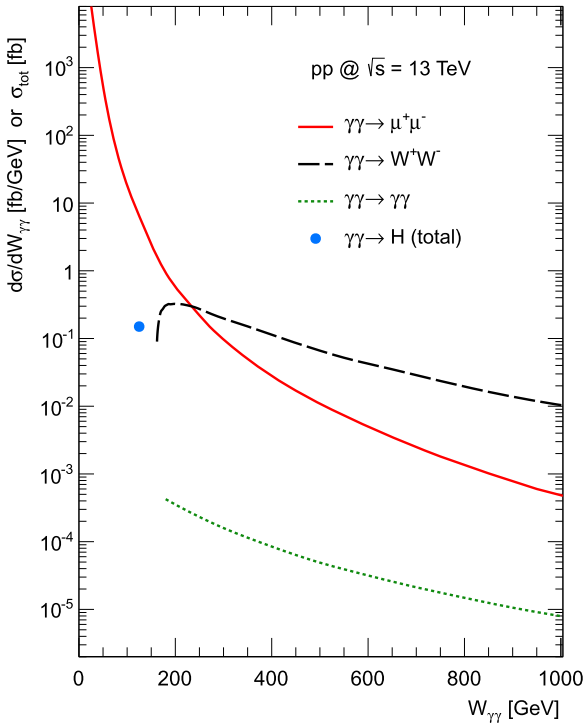

Fig. 1. Cross sections of various processes $pp(\gamma\gamma) \to ppX$, differential in the photon–photon center of mass energy. For the exclusive Higgs production, the total cross section is shown. The exclusive production of pairs of photons has been generated at large $W_{\gamma\gamma}$ where the cross section is dominated by one-loop diagrams involving W bosons.

This last dependence is not present in the approach based on formula (1). Following calculations presented in [15,16], the general equivalent photon distribution read

$$n(b,\omega) = \frac{\alpha_{EM}}{\pi^2\omega}\left|\int dk_\perp k_\perp^2 \frac{F\left(k_\perp^2 + \frac{\omega^2}{\gamma^2}\right)}{k_\perp^2 + \frac{\omega^2}{\gamma^2}} J_1(bk_\perp)\right|^2 \tag{2}$$

where γ is the Lorentz contraction factor, ω and $\vec{k}_\perp$ represent the energy and transverse momentum of photons respectively. In this expression, $F(.)$ is the proton form factor, electric and magnetic, that we develop explicitly below. Let us note that $n(b,\omega)$ depends only on the modulus of the impact parameter as obviously this quantity does not depend on the orientation of $\vec{b}$. We can introduce the virtuality of the photon $Q^2 = -k^2 = k_\perp^2 + \frac{\omega^2}{\gamma^2}$. Then, expression (2) becomes

$$n(b,\omega) = \frac{\alpha_{EM}}{\pi^2\omega}\left|\int dk_\perp k_\perp^2 \frac{F(Q^2)}{Q^2} J_1(bk_\perp)\right|^2, \tag{3}$$

After developing the complete expression of the form factor $F(.)$, we get

$$n(b,\omega) = \frac{\alpha_{EM}}{\pi^2\omega}\left|\int dk_\perp k_\perp^2 \frac{G_E(Q^2)}{Q^2} \times \left[(1-x)\frac{4m_p^2 + Q^2\mu_p^2}{4m_p^2 + Q^2} + \frac{1}{2}x^2\frac{Q^2}{k_\perp^2}\mu_p^2\right]^{\frac{1}{2}} J_1(bk_\perp)\right|^2, \tag{4}$$

where x is the energy fraction of the proton carried by the photon, given by $x = 2\omega/\sqrt{s}$. Let us note that the electromagnetic coupling strength α_{EM} is taken to be $\alpha_{EM}(Q^2 \simeq 0\ \text{GeV}^2) = 1/137.036$

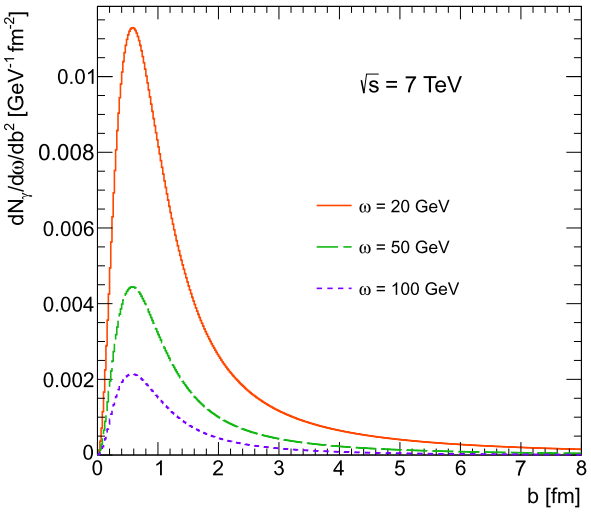

Fig. 2. Equivalent photon distributions of the fast moving proton for different energies of the photon, as function of the transverse distance b (see text).

throughout our calculations, following the property that the photons entering the interaction are quasi-real (see Section 1).

The relation (4) for $n(b,\omega)$ corresponds to the equivalent photon distribution (for one proton) when the impact parameter dependence is taken into account. Equivalent photon distributions are presented in Fig. 2, as a function of the impact parameter for different energies of the photon. The overall shapes of these distributions can be understood easily. At very large b values, $n(b,\omega)$ behaves asymptotically as $\frac{1}{b}e^{-2\omega b/\gamma}$ for what concerns its b dependence. At very small b values, the photon distributions are damped due to the effects of form factors and finite size of the proton. We can remark that Eq. (1) can be re-derived from expression (4) after replacing $f(\omega_1)$ by the integral of $n(\vec{b}_1,\omega_1)$ for all $\vec{b}_1$, and similarly for the second photon variables independently. Indeed

$$f(\omega)=\frac{e^2}{\pi\omega}\int\frac{d^2\vec{k}_\perp}{(2\pi)^2}\left(\frac{F\left(k_\perp^2+\frac{\omega^2}{\gamma^2}\right)}{k_\perp^2+\frac{\omega^2}{\gamma^2}}\right)^2|\vec{k}_\perp|^2,$$

where we have used the generic expression for the form factor of the proton, as in Eq. (2).

The full expression (4) is necessary when we want to take into account effects that depend directly on the transverse space variables of the reaction. Therefore, when we consider the finite sizes of colliding protons, we need to do the replacement

$$f(\omega_1)f(\omega_2)\to\iint n(\vec{b}_1,\omega_1)n(\vec{b}_2,\omega_2)d^2\vec{b}_1d^2\vec{b}_2, \tag{5}$$

where the bounds of integrations on the transverse distances $\vec{b}_1$ and $\vec{b}_2$ prevent from performing the integrations independently. Indeed, there are important geometrical constraints to encode: the two photons need to interact at the same point outside the two protons, of radii r_p, while the proton-halos do not overlap. This implies minimally that $b_1>r_p$, $b_2>r_p$ and $|\vec{b}_1-\vec{b}_2|>2r_p$ (see Fig. 3). The last condition clearly breaks the factorization in the variables $\vec{b}_1$ and $\vec{b}_2$ of the integral (5). In these conditions, the proton radius r_p is the two-dimensional radius, determined in the transverse plane, that will be taken to be 0.64 ± 0.02, as measured in the H1 experiment [17]. Let us note that it would be possible to keep the factorization by imposing stronger constraints, like $b_{1,2}>2r_p$. However, this last condition prevents configurations where the two protons are very close and produce very energetic photon–photon collisions. This is not what we want.

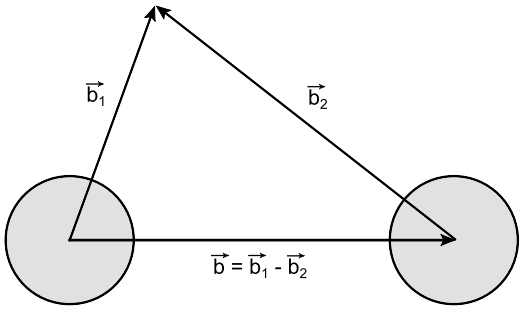

Fig. 3. Schematic view of the two protons and the transverse distances $\vec{b}_1$ and $\vec{b}_2$. The difference $\vec{b}=\vec{b}_1-\vec{b}_2$ is also pictured. This is clear from this view that the geometrical non-overlapping condition of the two protons corresponds to $|\vec{b}_1-\vec{b}_2|>2r_p$.

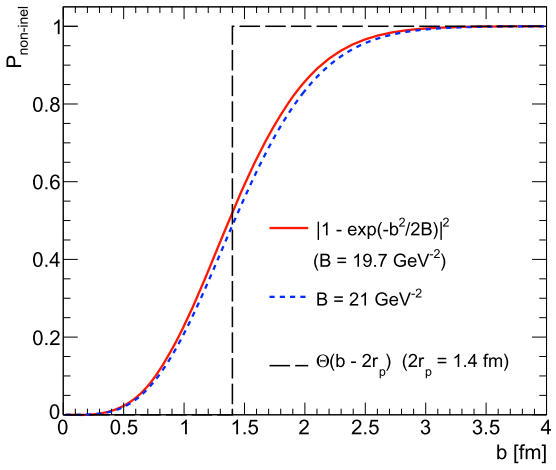

Fig. 4. Function $P_{non\text{-}inel}(b)=|1-\Gamma(b)|^2$ compared with the step function $\Theta(b-2R)$. $P(b)$ represents the probability for no inelastic interaction in a proton–proton collision at impact parameter b.

Eq. (5) is a first step towards encoding finite size effects. It can be refined by including the proton–proton interaction probability, which depends explicitly on the transverse variables, $P_{non\text{-}inel}(|\vec{b}_1-\vec{b}_2|)$. Then, Eq. (5) becomes

$$f(\omega_1)f(\omega_2)\to\iint n(\vec{b}_1,\omega_1)n(\vec{b}_2,\omega_2)P_{non\text{-}inel}\left(|\vec{b}_1-\vec{b}_2|\right)d^2\vec{b}_1d^2\vec{b}_2, \tag{6}$$

where the bounds of integrations are still $b_1>r_p$, $b_2>r_p$. The non-overlapping condition $|\vec{b}_1-\vec{b}_2|>2r_p$ is not needed any longer. It follows as a consequence of the effect of the function $P_{non\text{-}inel}(|\vec{b}_1-\vec{b}_2|)$. Indeed, this function represents the probability that there is no interaction (no overlap) between the two colliding protons in impact parameter space. Following [18], we make the natural assumption that a probabilistic approximation gives a reasonable estimate of the absorption effects. Then, we can write [18]

$$P_{non\text{-}inel}(b)=\left|1-\exp\left(-b^2/(2B)\right)\right|^2,$$

where the value of $B=19.7$ GeV^{-2} is taken from a measurement at $\sqrt{s}=7$ TeV by the ATLAS experiment [19] (see Fig. 4). At $\sqrt{s}=13$ TeV, we will use the extrapolated value $B=21$ GeV^{-2}. In Fig. 4, we compare $P_{non\text{-}inel}(b)$ with the step function $\Theta(b-2r_p)$, which is the first approximation that we have described above to quantify a non-overlapping condition between both protons. We see that both functions are roughly comparable. However, we can expect

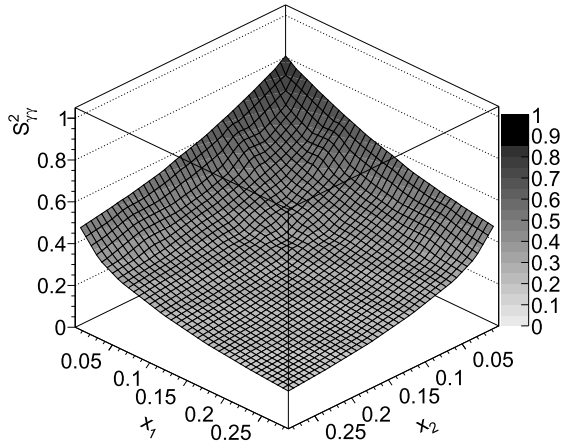

Fig. 5. The survival factor as a function of the energy fractions of the protons carried by the interacting photons, x_1 and x_2.

some deviations when performing more accurate computations of cross sections using $P_{non\text{-}inel}(b)$ in Eq. (6), and then in Eq. (1).

3. Results

Following the previous section, the first important issue is to quantify the size of the correction when we take into account the finite size of colliding protons. We define the survival factor as

$$S^2_{\gamma\gamma} = \frac{\int_{b_1>r_p}\int_{b_2>r_p} n(\vec{b}_1,\omega_1)n(\vec{b}_2,\omega_2)P_{non\text{-}inel}(|\vec{b}_1-\vec{b}_2|)d^2\vec{b}_1 d^2\vec{b}_2}{\int_{b_1>0}\int_{b_2>0} n(\vec{b}_1,\omega_1)n(\vec{b}_2,\omega_2)d^2\vec{b}_1 d^2\vec{b}_2}, \tag{7}$$

where the numerator contains the finite size effects encoded in the function $P_{non\text{-}inel}(b)$ and dedicated bounds of the integrations over $\vec{b}_1$ and $\vec{b}_2$, whereas the denominator represents the integral over all impact parameters with no constraint.

Trivially, this factor will always be smaller than unity. Then, the deviation with respect to unity will quantify the overestimation done when the finite size effects are neglected. This is first illustrated in Fig. 5, where we present the two-dimensional dependence of $S^2_{\gamma\gamma}$ as a function of x_1 and x_2, the energy fractions of the protons carried by the interacting photons. Then, the survival factor is displayed as a function of experimentally measurable variables in Figs. 6 and 7. Fig. 6 presents the behavior of the survival factor as a function of the center of mass energy of the photon–photon system ($W_{\gamma\gamma}$) at zero rapidity. Different curves are displayed corresponding to the different center of mass energies for the proton–proton collision. We observe a common feature. For all curves, the survival factor is decreasing as a function of $W_{\gamma\gamma}$, to reach values of 0.3 at $W_{\gamma\gamma} = 1$ TeV for $\sqrt{s} = 7$ or 8 TeV and 0.43 at $W_{\gamma\gamma} = 1$ TeV for $\sqrt{s} = 13$ TeV. This is a large effect, due to the fact that for larger values of $W_{\gamma\gamma}$, smaller values of $b = |\vec{b}_1 - \vec{b}_2|$ are probed, and thus the integral at the numerator of the survival factor (7) becomes smaller. Indeed, when the photon–photon energy becomes larger and larger, this is understandable that the probability of no inelastic interaction becomes smaller and smaller. Fig. 6 illustrates the behavior of the survival factor as a function of the rapidity of the photon–photon system, for different $W_{\gamma\gamma}$. Obviously, we observe the same effect as in Fig. 6, that when $W_{\gamma\gamma}$ increases the survival factor decreases. In addition, this figure shows the small dependence as a function of the rapidity $y_{\gamma\gamma}$. Let us note that for possible measurements at the LHC, the rapidity domain covered is close to zero. Therefore, the dependence in $y_{\gamma\gamma}$ is a marginal effect.

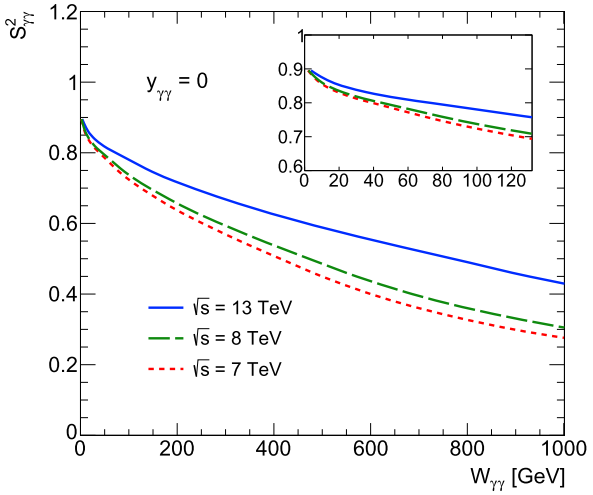

Fig. 6. The survival factor at zero rapidity as a function of the photon–photon center of mass energy.

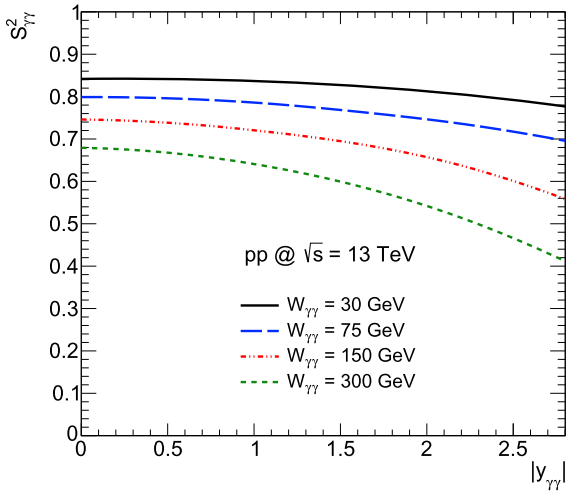

Fig. 7. The survival factor for different the photon–photon center of mass energies displayed as a function of the rapidity of the photon–photon system.

Table 1
Comparison of total cross sections at $\sqrt{s} = 13$ TeV for different processes $pp(\gamma\gamma) \to ppX$ with and without proton survival factor applied.

Process	σ_{tot}	$\sigma_{tot} \otimes S^2_{\gamma\gamma}$	$\langle S^2_{\gamma\gamma}\rangle$
$\gamma\gamma \to H$ ($M_H = 125$ GeV)	0.15 fb	0.11 fb	0.74
$\gamma\gamma \to \mu^+\mu^-$ ($W_{\gamma\gamma} > 40$ GeV)	12 pb	10 pb	0.8
$\gamma\gamma \to \mu^+\mu^-$ ($W_{\gamma\gamma} > 160$ GeV)	36 fb	25 fb	0.7
$\gamma\gamma \to W^+W^-$	82 fb	53 fb	0.65
$\gamma\gamma \to \gamma\gamma$ ($W_{\gamma\gamma} > 200$ GeV)	0.06 fb	0.04 fb	0.64

As a second step, we can compute cross sections for various processes $pp(\gamma\gamma) \to ppX$ taking correctly into account the finite size effects of incident protons and thus the survival factor. As discussed in the previous section, this requires Eq. (1) with the replacement (6). A set of predictions is presented in Table 1, where total cross sections are shown, cumulative in $W_{\gamma\gamma}$ above the bounds indicated in Table 1. For the exclusive production of pairs of W bosons, this is the natural bound which applies of $2M_W$.

Finally, we can compare our results with the experimental measurements available. Recently, the CMS experiment has measured exclusive pair of muons production [20] and has reported the value of $S^2_{\gamma\gamma}$ to be 0.83 ± 0.15 for invariant masses of the photon–

photon system above 11.5 GeV. This is consistent with our expectations from Fig. 6, which, convoluted with the elementary cross section in this kinematic range, gives a survival factor of 0.84. In addition, in the analysis of the exclusive production of pairs of W bosons by the CMS experiment [21], using exclusive muons production as a benchmark, the measured survival factor $S^2_{\gamma\gamma}$ is found to be about 10% smaller that the one above for invariant masses above 40 GeV. This is also consistent with our expectations ($S^2_{\gamma\gamma} = 0.76$ in this kinematic domain).

4. Conclusion

The exclusive production of a final state X, $pp(\gamma\gamma) \to ppX$, represents an essential class of reactions at the LHC, mediated through photon–photon interactions. The interest of such processes is due to their well-known initial conditions and simple final state. In this paper, we have presented a complete treatment of finite size effects of colliding protons, needed to compute the corresponding cross sections for these reactions. We have derived a survival factor that quantifies the deviation of the complete treatment with respect to no size effect.

We have shown that the survival factor is decreasing as a function of mass of the photon–photon system ($W_{\gamma\gamma}$), to reach values of 0.3 at $W_{\gamma\gamma} = 1$ TeV for $\sqrt{s} = 7$ or 8 TeV and 0.43 at $W_{\gamma\gamma} = 1$ TeV for $\sqrt{s} = 13$ TeV. This is a large effect, due to the fact that for larger values of $W_{\gamma\gamma}$, the probability of no inelastic interaction becomes smaller and smaller and so the survival factor. The key point of our approach is that it is valid for the full spectrum of invariant masses produced in the final state, and thus for high masses final states, like the production of a pair of W bosons or the Higgs boson. This allows a direct comparison with experimental results already obtained at the LHC beyond the electroweak scale, where a very good agreement has been observed between our expectations and the measurements.

Finally, we remind that these calculations are commonly used for the physics case of heavy-ion collisions. For example, this already exists with some approximations in the STARLIGHT Monte Carlo, mainly focused on the low invariant mass domain around the mass of the J/Ψ. A complication, properly taken into account in STARLIGHT, arises in such collisions, due to the large value of the charges of the ions. Then, photon–photon interactions may be accompanied by additional electromagnetic reactions, such as photo-nuclear interactions, and the ions that come out from the collisions may be produced with some neutrons.

Acknowledgements

This work was partly supported by the Polish National Science Centre under contract No. UMO-2012/05/B/ST2/02480.

References

[1] E. Fermi, Z. Phys. 29 (1) (1924) 315–327.
[2] E. Williams, Phys. Rev. 45 (1934) 729–730.
[3] M.S. Chen, I.J. Muzinich, H. Terazawa, T.P. Cheng, Phys. Rev. D 7 (1973) 3485.
[4] H. Terazawa, Rev. Mod. Phys. 45 (1973) 615.
[5] V. Budnev, I. Ginzburg, G. Meledin, V. Serbo, Nucl. Phys. B 63 (1973) 519–541.
[6] D. d'Enterria, M. Klasen, K. Piotrzkowski, Nucl. Phys. Proc. Suppl. 179B (2008) 1.
[7] J. de Favereau de Jeneret, V. Lemaitre, Y. Liu, S. Ovyn, T. Pierzchala, K. Piotrzkowski, X. Rouby, N. Schul, et al., arXiv:0908.2020 [hep-ph].
[8] M. Bahr, S. Gieseke, M.A. Gigg, D. Grellscheid, K. Hamilton, O. Latunde-Dada, S. Platzer, P. Richardson, et al., Eur. Phys. J. C 58 (2008) 639, arXiv:0803.0883 [hep-ph].
[9] M. Boonekamp, A. Dechambre, V. Juranek, O. Kepka, M. Rangel, C. Royon, R. Staszewski, arXiv:1102.2531 [hep-ph].
[10] S. Atag, S.C. Inan, I. Sahin, J. High Energy Phys. 1009 (2010) 042, arXiv:1005.4792 [hep-ph].
[11] M.A. Shifman, A.I. Vainshtein, M.B. Voloshin, V.I. Zakharov, Sov. J. Nucl. Phys. 30 (1979) 711;
B.A. Kniehl, M. Spira, Z. Phys. C 69 (1995) 77;
S. Dawson, R. Kauffman, Phys. Rev. D 49 (1994) 2298.
[12] A. Szczurek, Acta Phys. Pol. B 45 (2014) 7, arXiv:1404.0896 [nucl-th], 1597.
[13] S.R. Klein, J. Nystrand, Phys. Rev. Lett. 92 (2004) 142003, arXiv:hep-ph/0311164.
[14] R. Aaij, et al., LHCb Collaboration, J. Phys. G 40 (2013) 045001, arXiv:1301.7084 [hep-ex].
[15] M. Vidovic, M. Greiner, C. Best, G. Soff, Phys. Rev. C 47 (1993) 2308.
[16] A.J. Baltz, Y. Gorbunov, S.R. Klein, J. Nystrand, Phys. Rev. C 80 (2009) 044902, arXiv:0907.1214 [nucl-ex].
[17] F.D. Aaron, et al., H1 Collaboration, Phys. Lett. B 681 (2009) 391, arXiv:0907.5289 [hep-ex].
[18] L. Frankfurt, C.E. Hyde, M. Strikman, C. Weiss, Phys. Rev. D 75 (2007) 054009, arXiv:hep-ph/0608271.
[19] G. Aad, et al., ATLAS Collaboration, arXiv:1408.5778 [hep-ex].
[20] S. Chatrchyan, et al., CMS Collaboration, J. High Energy Phys. 1201 (2012) 052, arXiv:1111.5536 [hep-ex].
[21] S. Chatrchyan, et al., CMS Collaboration, J. High Energy Phys. 1307 (2013) 116, arXiv:1305.5596 [hep-ex].